TRANSIENT INTERNAL FORCED CONVECTION UNDER ARBITRARY TIME-DEPENDENT HEAT FLUX

M. Fakoor-Pakdaman
PhD Candidate,
mfakoorp@sfu.ca

M. Andisheh-Tadbir
PhD Candidate,
mandishe@sfu.ca

Majid Bahrami
Associate Professor,
mbahrami@sfu.ca

Laboratory for Alternative Energy Conversion (LAEC)
Mechatronic Systems Engineering,
School of Engineering Science,
Simon Fraser University,
Surrey, BC, Canada V3T 0A3

ABSTRACT

A new all-time model is developed to predict transient laminar forced convection heat transfer inside a circular tube under arbitrary time-dependent heat flux. Slug flow condition is assumed for the velocity profile inside the tube. The solution to the time-dependent energy equation for a step heat flux boundary condition is generalized for arbitrary time variations in surface heat flux using a Duhamel's integral technique. A cyclic time-dependent heat flux is considered and new compact closed-form relationships are proposed to predict: i) fluid temperature distribution inside the tube ii) fluid bulk temperature and iii) the Nusselt number. A new definition, cyclic fully-developed Nusselt number, is introduced and it is shown that in the thermally fully-developed region the Nusselt number is not a function of axial location, but it varies with time and the angular frequency of the imposed heat flux. Optimum conditions are found which maximize the heat transfer rate of the unsteady laminar forced-convective tube flow. We also performed an independent numerical simulation using ANSYS to validate the present analytical model. The comparison between the numerical and the present analytical model shows great agreement; a maximum relative difference less than 5.3%.

1. INTRODUCTION

For optimal design and accurate control of heat transfer in emerging sustainable energy applications and next-generation heat exchangers, it is crucial to develop an in depth understanding of thermal transients. Thermal transient may be accidental and random or may be of cyclic nature. Generally, processes such as start-up, shut-down, power surge, and pump/fan failure impose such transients [1–4].

Examples of thermal transient in sustainable energy applications include: i) the variable thermal load from thermal solar panels in Thermal Energy Storage (TES) systems; ii) the variable thermal load on power electronics of solar/wind/tidal energy conversion systems; and iii) the variable load of power electronics and electric motor of Hybrid Electric Vehicles (HEV), Electric Vehicles (EV), and Fuel Cell Vehicles (FCV). The following provides a brief overview on the importance and the trends of the above thermal engineering applications.

Solar thermal systems are widely utilized in solar power plants and are being widely commercialized. Solar power plants has seen about 740 MW of generating capacity added between 2007 and the end of 2010 bringing the global total to 1095 MW [4]. Such growth is expected to continue as in the US at least another 6.2 GW capacity is expected to be in operation by the end of 2013 [4]. However, the growth of such technology is hindered by the inherent variability of solar energy subjected to daily variation, seasonal variation, and weather conditions [1–3]. To overcome the issue of the intermittency, TES systems are used to collect thermal energy to smooth out the output and shift its delivery to a later time. Single-phase sensible heating systems or latent heat storage systems utilizing Phase Change Materials (PCM) are used in TES; transient heat exchange occurs to charge or discharge the

storage material. From the technical point of view, one of the main challenges facing TES systems is designing suitable heat exchangers to work reliably under unsteady conditions [1, 2], a key issue that this research attempts to address.

To assure reliable performance of electronic components, the temperature of different components should be maintained below recommended values. The temperature of power electronics can vary significantly with the fluid flow and the applied heat flux over time. Thus, it is important to investigate the transient thermal behavior of these systems, especially during peak conditions. Furthermore, new application of transient forced convection has emerged by the advent of HEV, EV, and FCV. Since introduced, the sales of such vehicles have grown at an average rate of more than 80% per year. As of October 2012, more than 5.8 million HEVs have been sold worldwide since their inception in 1997 [5]. Their hybrid powertrain and power electronics electric motors (PEEM) undergo a dynamic thermal load as a direct result of driving/duty cycle and environmental conditions. Conventional cooling systems are designed based on a nominal steady-state, typically a "worst" case scenario, which may not properly represent the thermal behavior of various applications or duty cycles. This clearly indicates the enormity of the pending need for in-depth understanding of the instantaneous thermal characteristics of the above-mentioned thermal systems. Successful and intelligent thermal design of such dynamic systems lead to the design of new efficient heat exchangers to enhance the overall efficiency and reliability of TES and PEEM cooling solutions, which in case of the HEV/EV/FCV means significant improvement in vehicle efficiency/reliability and fuel consumption [4–10].

In all the above-mentioned applications, transient heat transfer occurs in heat exchangers subjected to arbitrary time-dependent heat flux. This phenomenon can be represented by unsteady forced-convective tube flow, which is the ultimate goal of this study.

1.1. PERTINENT LITERATURE

Study on the transient forced-convective tube flow was begun by investigating the thermal response of the tube flow following a step change in wall heat flux or temperature. Sparrow and Siegel [12] conducted an analysis of transient heat transfer for fully developed laminar flow forced convection in the thermal entrance region of circular tubes. The unit step change in the wall heat flux or in the wall temperature was taken into account. Siegel and Sparrow [13] carried out a similar study in the thermal entrance region of flat ducts. Later Siegel [14] studied laminar slug flow forced convection heat transfer in a tube and a flat duct where the walls were given a step-change in the heat flux or alternatively a step-change in the temperature. The solution indicated that, for slug flow, steady state was reached in a wavelike fashion as fluid traveled downstream the channel from the entrance. Siegel [15] investigated transient laminar forced convection with fully developed velocity profile. It was shown that the slug flow

assumption revealed the essential physical behavior of the considered system. The periodic thermal response of channel flows to position- and time-dependent wall heat fluxes was also addressed in the literature. Siegel and Perlmutter [16] analyzed laminar forced convection heat transfer between two parallel plates with specific heat production. The heat production considered to vary with time and position along the channel. Some typical examples were considered for the heat production, and the tube wall temperature was evaluated for different specific cases. Perlmutter and Siegel [17] studied two-dimensional unsteady incompressible laminar duct flow between two parallel plates. Transient velocity was determined to account for the change in the fluid pumping pressure. An analytical-numerical study was carried out in Ref. [18] on the laminar forced convection in a flat duct with wall heat capacity and with wall heating variable with axial position and time. Most of the pertinent papers on transient forced convection are analytical-based; a summary of the literature is presented in Table 1.

Our literature review indicates:

- There is no model to predict the coolant behavior inside a conduit subjected to dynamic thermal load.
- The effects of a cyclic heat flux on the thermal performance of a tube flow are not investigated in the literature.
- There is no model to predict the Nusselt number of a tube flow under arbitrary time-dependent heat flux.
- There is no model to determine optimized condition that maximizes the heat transfer rate of transient forced-convective tube flow.

In this study, a new all-time model is developed to accurately predict: i) fluid temperature distribution inside the tube; ii) the fluid bulk temperature; and iii) the Nusselt number for a convective tube flow subjected to an arbitrary time-dependent heat flux. In most relevant papers [12–18], the transient thermal behavior of a system is evaluated based on the dimensionless wall heat flux, $\dot{Q}$, considering the difference between the local tube wall and the initial fluid temperature. In this study, however, a new local Nusselt number is defined based on the local temperature difference between the tube wall and the fluid bulk temperature at each axial location. We are of the opinion that our definition has a better physical meaning. Furthermore, a new definition, i.e. cyclic fully-developed Nusselt number, is introduced and it is shown that in the thermally fully-developed region the Nusselt number is not a function of axial location, but it varies with time and the characteristics of the imposed heat flux on the tube. In addition, optimum conditions are found to maximize the heat transfer rate of the tube flow under arbitrary time-dependent heat flux.

To develop the present analytical model the fluid flow response to a step heat flux is taken into account. A Duhamel's integral method is carried out on the thermal response of the fluid flow under the step heat flux, following Ref. [14]. A cyclic time-dependent heat flux is taken into consideration, and the thermal characteristics of the fluid flow are determined analytically under such heat flux boundary conditions. Any type

of time-dependent heat flux can be decomposed into simple oscillatory functions using a Fourier series transformation. Thus, the results of this study can be readily applied to determine the transient fluid flow response under a dynamically varying heat flux.

Table 1: Summary of the existing analytical models for unsteady, internal convective heat transfer

Author	Boundary condition and velocity profile	Geometry	Notes
Sparrow and Siegel [12]	Step wall temperature/ heat flux Fully developed flow	Circular duct	Algebraic expressions to find the tube wall temperature/heat flux.
Siegel and Sparrow [13]	Step wall temperature/heat flux Fully developed flow	Flat duct	Algebraic expressions to find the tube wall temperature/heat flux.
Siegel [14]	Step wall temperature/ heat flux Slug flow	Circular/flat duct	Series solutions to find the temperature distribution inside the fluid.
Siegel [15]	Step wall temperature Fully developed flow	Circular duct	Series solutions to find the temperature distribution inside the fluid.
Siegel and Perlmutter [16]	Time-dependent heat flux Slug /transient flow	Flat duct	Reported temperature distribution inside the fluid.
Perlmutter and Siegel [17]	Step wall temperature Fully-developed flow	Flat duct	Evaluated tube wall temperature considering the tube wall thermal inertia.
Siegel [18]	Time-dependent heat flux Slug flow	Flat duct	Evaluated tube wall temperature considering the tube wall thermal inertia.

2. GOVERNING EQUATIONS

Figure 1 shows a circular tube of diameter D which is thermally insulated in the first sub-region, $x \leq 0$, and is heated in the second sub-region, $x > 0$. The tube and fluid are assumed to be initially isothermal at temperature T_0. The entering fluid temperature is also maintained at T_0 throughout the heating period. The wall at the second sub-region is given an arbitrary time-dependent heat flux, $q''(t)$. It is also assumed that the entering fluid temperature and the first sub-region are maintained at T_0 throughout the heating period. It should be noted that the second sub-region may be long enough so that the fluid flow can reach thermally fully developed condition along this section, see Fig. 1. It is intended to determine the evolution of the tube wall temperature, fluid bulk temperature and the Nusselt number as a function of time and space for the entire range of the Fourier number under arbitrary time-dependent heat flux.

The energy equation for a fluid flowing inside a circular duct in this instance is shown by Eq. (1):

$$\frac{\partial T}{\partial t} + u \frac{\partial T}{\partial x} = \alpha \frac{1}{r} \frac{\partial}{\partial r} \left(r \frac{\partial T}{\partial r} \right) \tag{1}$$
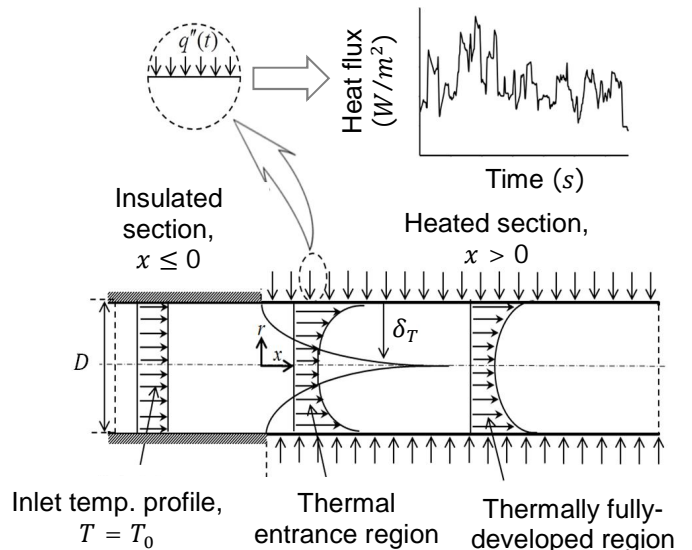

Figure 1. Schematic of the two-region tube and the coordinate system.

For the case of Slug Flow (SF), see Section 3 for more detail, the velocity distribution and the energy equation can be written as follows:

$$u(r, x, t) = U = const. \tag{2}$$

$$\frac{\partial \theta}{\partial Fo} + \frac{\partial \theta}{\partial X} = \frac{1}{\eta}\frac{\partial}{\partial \eta}\left(\eta \frac{\partial \theta}{\partial \eta}\right) \qquad (3)$$

The dimensionless variables are defined as follows:

$$Fo = \frac{\alpha t}{R^2} \qquad X = \frac{4x/D}{\mathrm{Re.Pr}} \qquad \theta = \frac{T - T_0}{q_r''D/k} \qquad \eta = \frac{r}{R}$$

where Fo is the Fourier number and X is the dimensionless axial location that characterizes the flow inside a conduit, respectively.

As previously mentioned, the final goal of this study is to find the transient thermal response of forced-convective tube flow under an arbitrary time-dependent heat flux. Therefore, a general prescribed heat flux is assumed as follows:

$$q''(Fo) = q_r''.\varphi(X, Fo) \qquad (4)$$

where q_r'' is the heat flux amplitude and $\varphi(X, Fo)$ is an arbitrary function of space and time, respectively.
Consequently, Eq. (4) is subjected to the following initial and boundary conditions:

$\theta(X, \eta, 0) = 0$ Initial condition,

$\theta(0, \eta, Fo) = 0$ Entrance condition,

$(\partial \theta / \partial \eta)\big|_{\eta=1} = \frac{1}{2}\varphi(X, Fo)$ Heat flux at the tube wall for $Fo > 0$,

$(\partial \theta / \partial \eta)\big|_{\eta=0} = 0$ Symmetry at the center line.   (5)

3. MODEL DEVELOPMENT

In this section, a new all-time model is developed considering; i) short-time response and ii) long-time response. The following assumptions are made:

- Incompressible flow,
- Constant thermo-physical properties,
- Negligible viscous dissipation,
- Negligible axial heat conduction,
- No thermal energy sources within the fluid,
- Uniform velocity profile along the tube, i.e., slug flow.

Slug flow assumption can predict the thermal behavior of any type of fluid flow close to the tube entrance where the velocity profile is developing and has not reached the fully developed condition [14], [18]. We plan to study the transient thermal response of the tube flow with fully developed velocity profile under dynamically varying heat flux in the

future. When a cylinder at uniform temperature T_0 is suddenly subjected to a step heat flux $\Delta q''$ at its surface, the temperature response is [14]:

$$\theta_s = \frac{T_w - T_0}{q_r''D/k} = \frac{\Delta q''}{q_r''}\left[Fo + \frac{2\eta^2 - 1}{8} - \sum_{n=1}^{\infty} e^{-\beta_n^2 Fo}\frac{J_0(\beta_n \eta)}{\beta_n^2 J_0(\beta_n)}\right] \quad (6)$$

where θ_s is the dimensionless temperature of the fluid under a step heat flux, β_n are the positive roots of $J_1(\beta) = 0$, and $J_1(\beta)$ are the Bessel functions of the first kind, respectively. The energy equation for a tube flow is linear, i.e., Eq. (1). This shows the applicability of a superposition technique to extend the response of the fluid flow for a step heat flux to the other general cases as discussed in [16]. As such, by using Duhamel's integral [19], the thermal response for a step heat flux, Eq. (6), can be generalized for an arbitrary time variations in surface heat flux.

$$\theta = \int_0^{Fo} \frac{q''(\xi)}{q_r''}d\xi + \sum_{n=1}^{\infty} e^{-\beta_n^2 Fo}\frac{J_0(\beta_n \eta)}{J_0(\beta_n)}\int_0^{Fo} e^{\beta_n^2 \xi}\frac{q''(\xi)}{q_r''}d\xi \quad (7)$$

This expression is only valid when the element is initially isothermal, so the treatment here is limited to the cases where the channel is initially isothermal. However, the extension to the other cases can be achieved by superposition techniques, as discussed in [16].

As shown in Fig. 2, in the Eulerian coordinate system, the observer is fixed at a given location x along the tube and the fluid moves by.
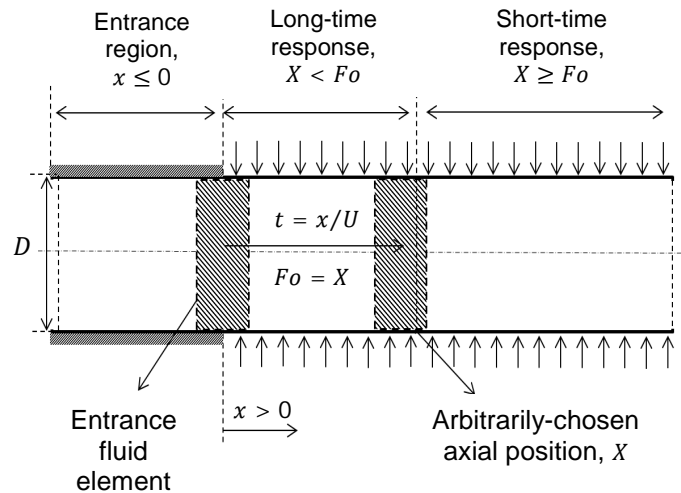

Figure 2. The methodology adopted to find the transient thermal response of the tube flow under arbitrary time-dependent heat flux.

It will take some time, $t = x/U, Fo = X$, for the entrance fluid to reach the axial position X. Beyond this distance region, $X \geq Fo$, there has not been any penetration of the

fluid which was originally outside the tube when the transient began. Therefore, the heat-flow process in this region is not affected. Hence, the behavior in this region is then that of a tube with infinite length in both directions. This means that the convective term in the energy equation, Eq. (1), is identically zero and a pure transient "heat-conduction" process takes place. On the other hand, for $X < Fo$ the observer situated at X will see the passing fluid which was in the entrance region, insulated section, when the transient was initiated. This is considered as the long-time response of the fluid flow [16]. Therefore, the solution consists of two regions that should be considered separately. The methodology considered in this study is shown schematically in Fig. 2.

3.1. SHORT-TIME RESPONSE, $X \geq Fo$

For the sake of generality, we consider a case in which the heat flux varies with both time and space, $q''(X, Fo)$. We first consider the region where $X \geq Fo$. A fluid element that reaches X at time Fo was already in the heated section at the location $X - Fo$ at the beginning of the transient. As this element moves along, it is subjected to the heat flux variations in both time and space. At a time ξ between 0 and Fo, the element is arrived to the location $X - Fo + \xi$. Thus, the heat flux that the element is subjected to at that time is $q''(X - Fo + \xi, \xi)$. This is substituted into Eq. (7) to find the short-time response for the fluid temperature distribution [16].

$$\theta(X, Fo) = \int_0^{Fo} \frac{q''(X - Fo + \xi, \xi)}{q_r''} d\xi +$$
$$\sum_{n=1}^{\infty} e^{-\beta_n^2 Fo} \frac{J_0(\beta_n \eta)}{J_0(\beta_n)} \int_0^{Fo} e^{\beta_n^2 \xi} \frac{q''(X - Fo + \xi, \xi)}{q_r''} d\xi \quad (8)$$

It should be noted that according to Eq. (8) when the imposed heat flux is only a function of time, $q'' = q''(Fo)$, the short-time thermal response of the fluid flow is not dependent upon the axial position. However, it is a function of time and the characteristics of the imposed heat flux.

3.2. TRANSITION TIME, $X = Fo$

For each axial position, the short-time and long-time responses are equal at $X = Fo$. This is the dimensionless transition time for a given axial position. Therefore, the time $Fo = X$ is a demarcation between the short-time and long-time responses for each axial position. For instance, for an arbitrarily-chosen axial position $X = 0.4$, the dimensionless transition time is $Fo = 0.4$. This arbitrary example will be used throughout the analysis in this paper.

3.3. LONG-TIME RESPONSE, $X < Fo$

Now we consider the region, where $X < Fo$. The element that reaches X at time Fo, entered the channel at the time

$Fo - X$ and began to be heated. As time elapses from when the transient begins, this element will reach the location ζ at the time $Fo - X + \zeta$. Thus, the heat flux that the element is subjected to at that location is $q''(\zeta, Fo - X + \zeta)$. Substituting this into Eq. (7) results in Eq. (9), which represents the long-time response of the flow at each axial position.

$$\theta(X, Fo) = \int_0^X \frac{q''(\zeta, Fo - X + \zeta)}{q_r''} d\zeta +$$
$$\sum_{n=1}^{\infty} e^{-\beta_n^2 X} \frac{J_0(\beta_n \eta)}{J_0(\beta_n)} \int_0^X e^{\beta_n^2 \zeta} \frac{dq''(\zeta, Fo - X + \zeta)}{q_r''} d\zeta \quad (9)$$

According to Eq. (9), the long-time thermal response of the fluid flow is a function of time, axial position and the characteristics of the imposed heat flux.

4. CYCLIC THERMAL TRANSIENTS

Any type of prescribed time-dependent heat flux can be decomposed into periodic functions as the summation of a set of simple oscillating functions, namely sines and cosines by Fourier series. As such, we develop the present model for a cyclic heat flux, and the results can be generalized to cover the cases with arbitrary time variations in surface heat flux by using a superposition technique.

The following expression is considered as a cyclic heat flux imposed on the tube wall,

$$q''(\omega, Fo) = q_r'' \left[1 + \sin(\omega Fo) \right] \quad (10)$$

where ω is the angular frequency of the imposed heat flux which characterizes the behavior of the prescribed cyclic heat flux.

The following compact relationship is developed in this study to present the temperature distribution inside the fluid in a compact form with a maximum relative difference of 1%.

$$\sum_{n=1}^{\infty} \frac{J_0(\beta_n \eta)}{\beta_n^2 J_0(\beta_n)} = \frac{2\eta^2 - 1}{8} \quad (11)$$

After substituting Eq. (10) into Eqs. (8) and (9), we take Eq. (11) into account, and the short-time and long-time temperature distribution inside the fluid are obtained. In this study we considered the first 60 terms of the series solutions.

Short-time response, $X \geq Fo$:

$$\theta(\omega, Fo) = Fo + \frac{1}{\omega} \times \left[1 - \cos(\omega Fo) \right] + \frac{2\eta^2 - 1}{8} -$$
$$\sum_{n=1}^{\infty} \frac{J_0(\beta_n \eta)}{J_0(\beta_n)} \times \left\{ \begin{array}{l} \dfrac{e^{-\beta_n^2 Fo}}{\beta_n^2} + \dfrac{\omega}{\omega^2 + \beta_n^4} \times \\ \left[\cos(\omega Fo) - \dfrac{\beta_n^2}{\omega} \times \sin(\omega Fo) - e^{-\beta_n^2 Fo} \right] \end{array} \right\} \quad (12)$$

Long-time response, $X < Fo$:

$$\theta(\omega, X, Fo) = X + \frac{1}{\omega} \times \left\{ \cos\left[\omega(Fo-X)\right] - \cos(\omega Fo) \right\} +$$

$$\frac{2\eta^2 - 1}{8} - \sum_{n=1}^{\infty} \frac{J_0(\beta_n \eta)}{J_0(\beta_n)} \times \left\{ \begin{array}{l} \dfrac{e^{-\beta_n^2 X}}{\beta_n^2} + \dfrac{\omega}{\omega^2 + \beta_n^4} \times \\ \left[\cos(\omega Fo) - \dfrac{\beta_n^2}{\omega} \times \sin(\omega Fo) + \right. \\ \left. e^{-\beta_n^2 X} \times \left\{ \dfrac{\beta_n^2}{\omega} \times \sin\left[\omega(Fo-X)\right] - \right. \right. \\ \left. \left. \cos\left[\omega(Fo-X)\right] \right\} \right] \end{array} \right\} \quad (13)$$

In addition, the tube-wall temperature can be defined by evaluating Eqs. (12) and (13) at $\eta = 1$. Since using the above series solution is tedious, the following new compact, easy-to-use relationships are developed in this study to predict the short-time and long-time tube-wall temperatures.

Short-time tube-wall temperature, $X \geq Fo$:

$$\theta_w(\omega, Fo) = Fo + \frac{1}{\omega} \times \left[1 - \cos(\omega Fo)\right] + \frac{1}{8}$$
$$- 0.086 \times \exp(-16.8 Fo) + 0.078 \times \sin(\omega Fo - 6.75) \quad (14)$$

Long-time tube-wall temperature, $X < Fo$:

$$\theta_w(\omega, X, Fo) = X + \frac{1}{\omega} \times \left\{ \cos\left[\omega(Fo-X)\right] - \cos(\omega Fo) \right\}$$
$$+ \frac{1}{8} - 0.086 \times \exp(-16.8 X) + 0.078 \times \sin(\omega Fo - 6.75) \quad (15)$$

The maximum and average relative difference of the values predicted by Eqs. (14) and (15) compared with the exact values obtained by Eqs. (12) and (13) are 6.1 and 2.1%, respectively. In addition, the fluid bulk temperature can be obtained by performing a heat balance on an infinitesimal differential control volume of the flow:

$$\dot{m} c_p T_m + q''(\pi D) dx - \left(\dot{m} c_p T_m + \dot{m} c_p \frac{\partial T_m}{\partial x} dx \right) =$$
$$\rho c_p \left(\frac{\pi D^2}{4} \right) \frac{\partial T_m}{\partial t} dx \quad (16)$$

The dimensionless form of Eq. (16) is:

$$\frac{q''(X, Fo)}{q_r''} = \frac{\partial \theta_m}{\partial Fo} + \frac{\partial \theta_m}{\partial X} \quad (17)$$

Equation (17) is a first-order partial differential equation which can be solved by the method of characteristics [19]. The short-time and long-time fluid bulk temperatures can be obtained as follows.

$$\theta_m(\omega, Fo, X) = \begin{cases} Fo + \dfrac{1}{\omega}\left[1 - \cos(\omega Fo)\right] & X \geq Fo \\ X + \dfrac{1}{\omega}\left\{\cos\left[\omega(Fo-X)\right] - \cos(\omega Fo)\right\} & X < Fo \end{cases} \quad (18)$$

In this study, the local Nusselt number is defined based on the difference between the tube-wall and fluid bulk temperatures.

$$Nu_D = \frac{q''D/k}{T_w - T_m} = \frac{\varphi(X, Fo)}{\theta_w - \theta_m} = \frac{1 + \sin(\omega Fo)}{\theta_w - \theta_m} \quad (19)$$

where θ_w and θ_m are the dimensionless wall and fluid bulk temperatures obtained previously, Eqs. (12), (13), and (18), respectively. Therefore, the short-time and long-time Nusselt numbers are obtained as follows:

Short-time Nusselt number, $X \geq Fo$:

$$Nu_D(\omega, Fo) =$$
$$\frac{1 + \sin(\omega Fo)}{\dfrac{1}{8} - \sum\limits_{n=1}^{\infty} \left\{ \begin{array}{l} \dfrac{e^{-\beta_n^2 Fo}}{\beta_n^2} + \dfrac{\omega}{\omega^2 + \beta_n^4} \times \\ \left[\cos(\omega Fo) - \dfrac{\beta_n^2}{\omega} \times \sin(\omega Fo) - e^{-\beta_n^2 Fo} \right] \end{array} \right\}} \quad (20)$$

Long-time Nusselt number, $X < Fo$:

$$Nu_D(\omega, X, Fo) =$$
$$\frac{1 + \sin(\omega Fo)}{\dfrac{1}{8} - \sum\limits_{n=1}^{\infty} \left\{ \begin{array}{l} \dfrac{e^{-\beta_n^2 X}}{\beta_n^2} + \dfrac{\omega}{\omega^2 + \beta_n^4} \times \\ \left[\cos(\omega Fo) - \dfrac{\beta_n^2}{\omega} \times \sin(\omega Fo) + \right. \\ \left. e^{-\beta_n^2 X} \times \left\{ \dfrac{\beta_n^2}{\omega} \times \sin\left[\omega(Fo-X)\right] - \right. \right. \\ \left. \left. \cos\left[\omega(Fo-X)\right] \right\} \right] \end{array} \right\}} \quad (21)$$

Using the compact relationships developed for the tube and wall temperatures, i.e. Eqs. (14) and (15), the local Nusselt number can also be calculated by the following compact closed-form relationships.

6

Short-time Nusselt number, $X \geq Fo$:

$$Nu_D(\omega, Fo) =$$

$$\frac{1 + \sin(\omega Fo)}{\frac{1}{8} + 0.078 \times \sin(\omega Fo - 6.75) - 0.086 \times \exp(-16.8 Fo)} \quad (22)$$

Long-time Nusselt number, $X < Fo$:

$$Nu_D(\omega, X, Fo) =$$

$$\frac{1 + \sin(\omega Fo)}{\frac{1}{8} + 0.078 \times \sin(\omega Fo - 6.75) - 0.086 \times \exp(-16.8 X)} \quad (23)$$

For $Fo > 0.05$, Eqs. (22) and (23) predict the exact results, Eqs. (20) and (21), with the maximum and average relative difference of 10 and 4%, respectively.

For $X > 0.2$, $\omega > 8\pi$ the long-time Nusselt number, Eq. (23), can be written as follows:

$$Nu_D(\omega, Fo) = \frac{1 + \sin(\omega Fo)}{\frac{1}{8} + 0.078 \times \sin(\omega Fo - 6.75)} \quad (24)$$

As discussed later in Section 6, this is the cyclic fully-developed Nusselt number for $X \geq 0.2$ which is not a function of the axial position. However, it varies arbitrarily with time and the angular frequency. Since the local Nusselt number is a function of both time and space, the average Nusselt number for an arbitrarily chosen time-interval between 0 and Fo is defined as follows:

$$\overline{Nu}_D(\omega) = \frac{1}{Fo \times X} \int_{\xi=0}^{Fo} \int_{\zeta=0}^{X} Nu_D \, d\zeta \, d\xi \quad (25)$$

5. NUMERICAL STUDY

To validate the proposed analytical model, an independent numerical simulation of the axisymmetric flow inside a circular tube is done using the commercial software, ANSYS® Fluent [20]. A user defined code (UDF) is written to apply the dynamic heat flux on the tube wall, Eq. (10). Furthermore, the assumptions stated in Section 3 are used in the numerical analysis, however, the fluid axial conduction is not neglected in the numerical analysis. Grid independence is tested for different cases and the size of computations grids is selected such that the maximum difference in the predicted values for the fluid temperature is less than 2%. Water is selected as the working fluid for the numerical simulations. The maximum relative difference between the analytical results and the numerical data is less than 5.3%, which are discussed in detail in Section 6.

6. RESULTS AND DISCUSSION

Throughout this study, the results are represented for an arbitrarily-chosen axial position of $X = 0.4$; the results for other axial positions are similar. Variations of the dimensionless tube wall temperature against the Fo number, Eqs. (14) and (15), for a few axial positions along the tube are shown in Fig. 3, and compared with the numerical data obtained in Section 5 of this study.

As shown in Fig. 3,
- There is an excellent agreement between the analytical results Eqs. (14),(15) and the numerical data over the short-time response. However, there is a small discrepancy between the numerical data and analytical results in the long-time response region, $X < Fo$. The maximum relative difference between the present analytical model and the numerical data is less than 5.3%.
- The present model predicts an abrupt transition between the short-time and long-time responses. The numerical results, however, indicate a smoother transition between the responses. This causes the numerical data to deviate slightly from the analytical results as the long-time response begins.
- There is an initial transient period of pure conduction during which all of the curves follow along the same line, $X \geq Fo$.
- When $Fo = X$, each curve moves away from the common line i. e. pure conduction response and adjusts towards a steady oscillatory behavior at long-time response, Eq. (15). The wall temperatures become higher for larger X values, as expected, because of the increase in the fluid bulk temperature in the axial direction.
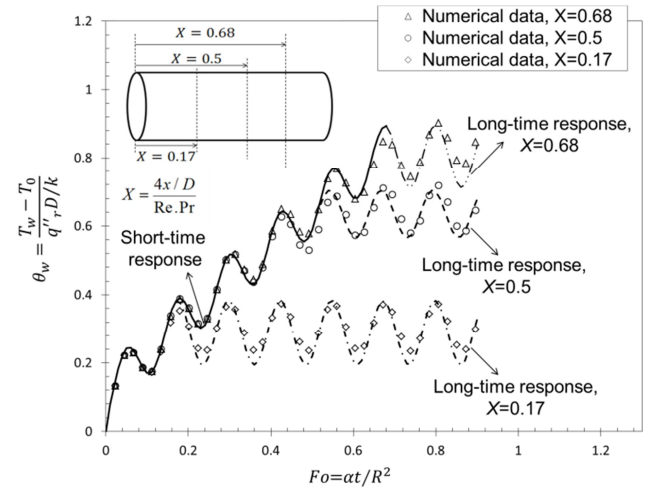

Figure 3. Variations of the dimensionless tube wall temperature versus the *Fo* number at $X = 0.4$ for a cyclic heat flux $q'' = q''_r \left[1 + \sin(8\pi Fo) \right]$.

Figure 4 shows the variations of the dimensionless fluid temperature at different radial positions across the tube versus the *Fo* number, Eqs. (12) and (13). Step heat flux, i.e. when $\omega \to 0$, and cyclic heat flux with angular frequency fixed at an arbitrarily-chosen value of 8π, are considered. As such, the short-time and long-time fluid temperature at different radial positions at an arbitrarily-chosen axial position, $X = 0.4$, are obtained using Eqs. (12) and (13).

From Fig. 4, the following conclusions can be drawn:
- As expected at any given axial position, the fluid temperature oscillates with time in case of a cyclic heat flux. For a step heat flux, the solution does not fluctuate over time.
- At any given axial position, there is an initial transient period, which can be considered as pure conduction, i.e., the short-time response for $X \geq Fo$. However, as pointed out earlier, each axial position shows steady oscillatory behavior for $X < Fo$ at the long-time response. Therefore, for the arbitrarily-chosen axial position of $X = 0.4$, the long-time response begins at $Fo = 0.4$, and shows the same behavior all-time thereafter.
- For a cyclic heat flux, the fluid temperature oscillates around the associated response for the step heat flux with the same magnitude.
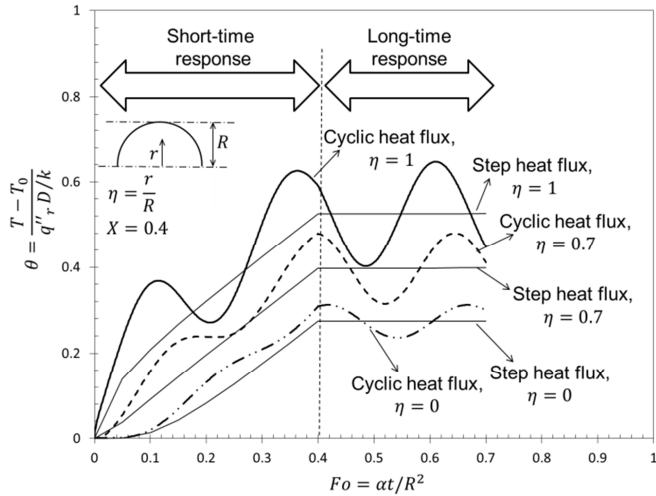

Figure 4. Variations of the dimensionless fluid temperature at an arbitrarily-chosen axial position of $X = 0.4$ and angular frequency of 8π at different radial positions across the tube against the *Fo* number for cyclic and step heat fluxes.

Figure 5 shows the long-time tempearture distribution inside the fluid at a given axial position of $X = 0.4$, at different radial positions for a cyclic heat flux with the angular frequency fixed at $\omega = 8\pi$, Eq. (13).

One can conclude the following from Fig. 5:
- The shift between the peaks of the temperature profile is marked at different radial positions. This shows a "thermal lag" (inertia) of the fluid flow, which increases towards the centerline of the tube. This thermal lag is attributed to the fluid thermal inertia.
- Considering Eq. (13), the maximum temperature inside the fluid for different radial positions at an arbitrarily-chosen axial position, $X = 0.4$, can be found as follows for $0.5 \leq Fo \leq 0.8$. Obviously, the same approach can be applied to other axial locations.

$$\frac{d\theta}{dFo}\Big|_{X=0.4} = 0 \Rightarrow \theta_{max} = -5.5 \times Fo + 3.995$$
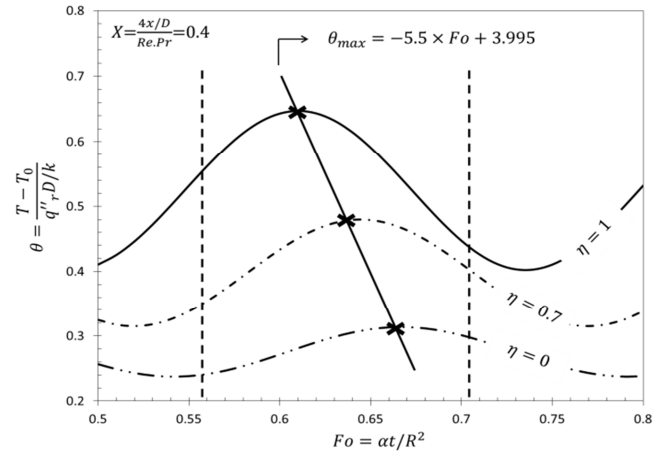

Figure 5. Peak-shifting trend of maximum long-time temperatures inside the fluid at different radial positions at an arbitrarily-chosen axial position of $X = 0.4$ and angular frequency of 8π.

Figure 6 shows the variations of the dimensionless tube-wall temperature at a given axial position of $X = 0.4$, versus the Fourier number and the angular frequency, Eqs. (14) and (15).

The followings can be concluded from Fig. 6:
- At the two limiting cases where: i) $\omega \to 0$ and ii) $\omega \to \infty$, the fluid flow response yields that of a step heat flux.
- When a sinusoidal cyclic heat flux with high angular frequency is imposed on the flow, the fluid does not follow the details of the heat flux behavior. Therefore, for very high angular frequencies, the fluid flow acts as if the imposed heat flux is constant at "the average value" associated with zero frequency for the sinusoidal heat flux in this case.
- The tube wall temperature can deviate considerably from that of the step heat flux at the small values of the angular frequency, i.e. $2 < \omega < 11 (rad)$.

- The conventional way to decrease the wall temperature of heat exchangers is to cool down the working fluid. However, it is shown that changing the heat flux frequency can also dramatically alter the tube wall temperature.
- The highest temperature for the tube wall occurs for small values of angular frequency. Considering Eq. (15), the highest long-time tube wall temperature occurs at

$$\frac{d\theta_w}{d\omega} = 0 \Rightarrow \omega \approx 1.7 \, (rad).$$

- Irrespective of Fo number, the amplitude of the dimensionless tube wall temperature decreases remarkably as the angular frequency increases. As mentioned earlier, this happens due to the fact that for high angular frequencies the fluid flow response approaches to that of the step heat flux.
- At a given axial position, the maximum long-time tube wall temperature is remarkably higher than that of short-time response.
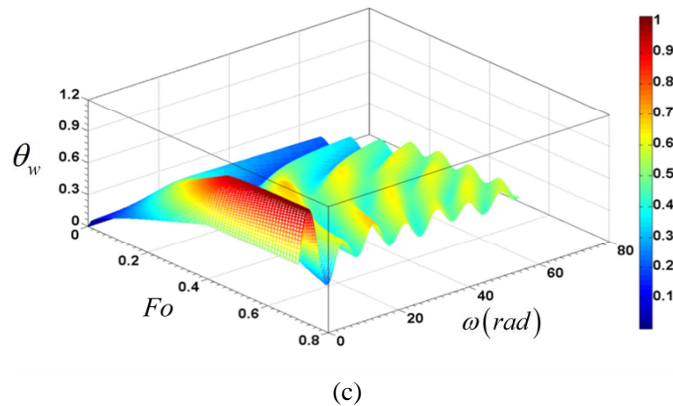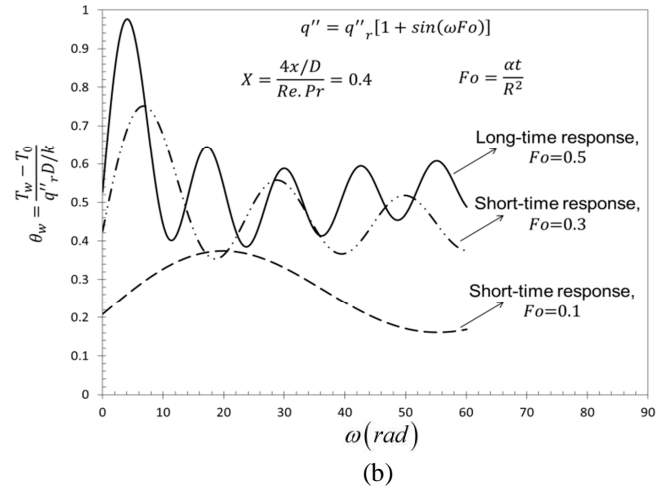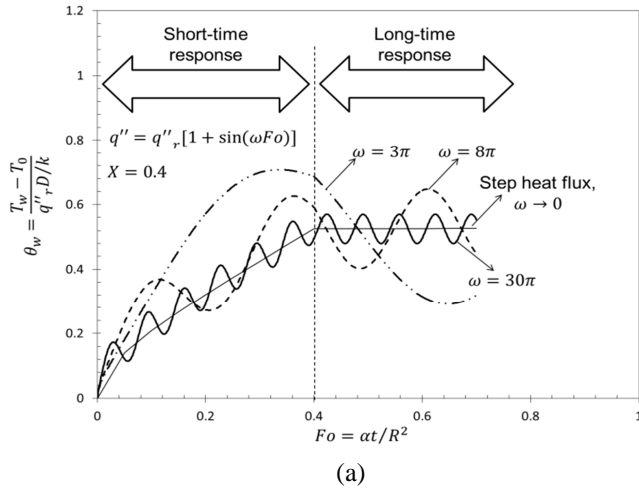

(a)

(b)

(c)

Figure 6: Variations of the dimensionless tube-wall temperature at an arbitrarily-chosen axial position of $X = 0.4$ against (a): the Fourier number for different angular frequencies of the heat flux, (b) the angular frequency at different Fourier numbers, and (c) the angular frequency and the Fourier number.

Figure 7 shows the variations of the dimensionless fluid bulk temperature at a given arbitrary axial position of $X = 0.4$, versus the Fourier number and the angular frequency, Eq. (18).

From Fig. 7, one can conclude:
- Irrespective of Fo number, the amplitude of the dimensionless fluid bulk temperature decreases remarkably as the angular frequency increases.

- The fluctuations of the fluid bulk temperature at high angular frequencies are small compared to that of the tube wall temperature.
- Comparing Figs. 6 and 7, the fluid bulk temperature shows a similar behavior as the tube wall temperature with the Fourier number and the angular frequency. However, as expected at each axial position, the fluid bulk temperature is less than the tube-wall temperature regardless of the angular frequency and Fo number.
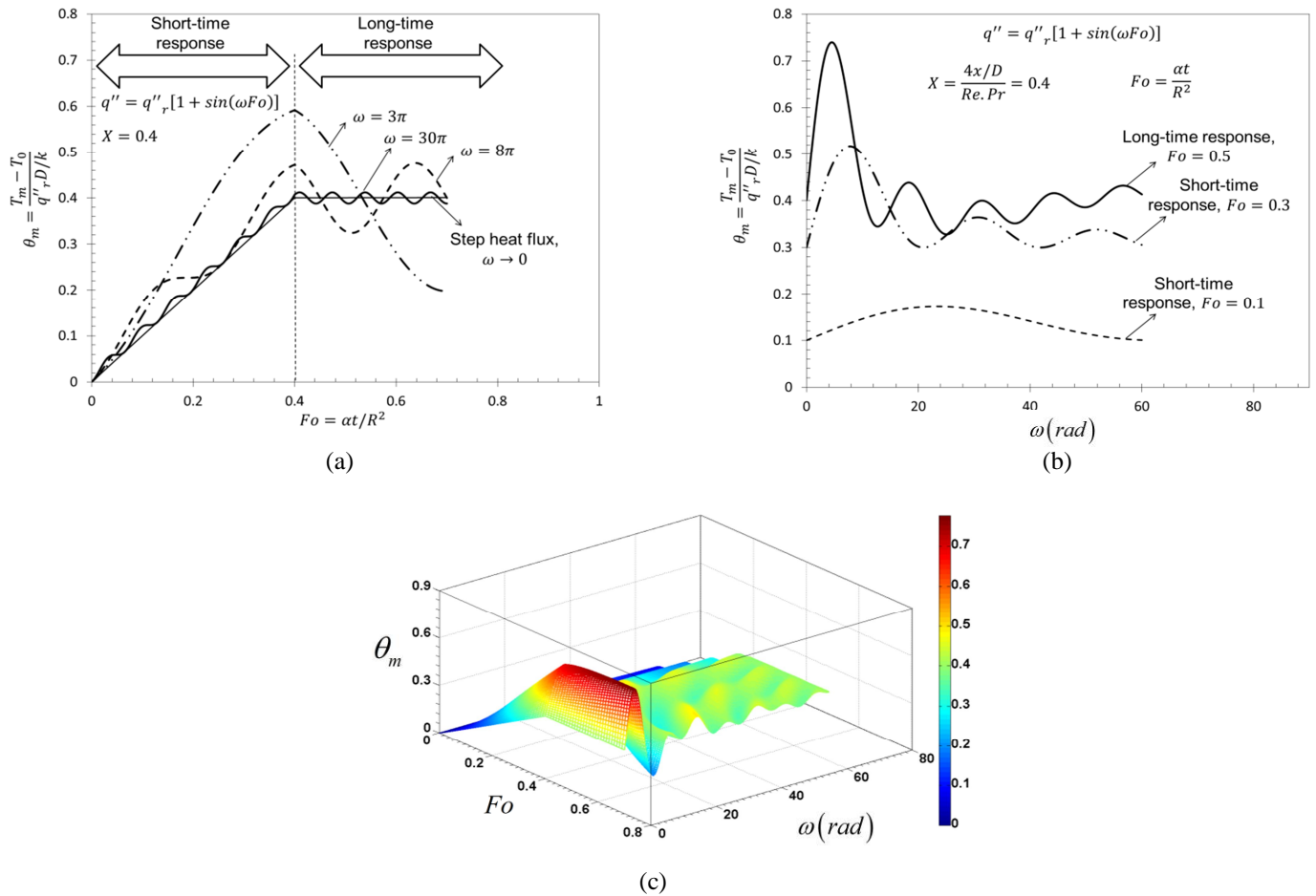
Figure 7: Variations of the dimensionless fluid bulk temperature at an arbitrarily-chosen axial position of $X = 0.4$ against (a): the Fourier number for different angular frequencies of the heat flux, (b) the angular frequency at different Fourier numbers, and (c) the angular frequency and the Fourier number.
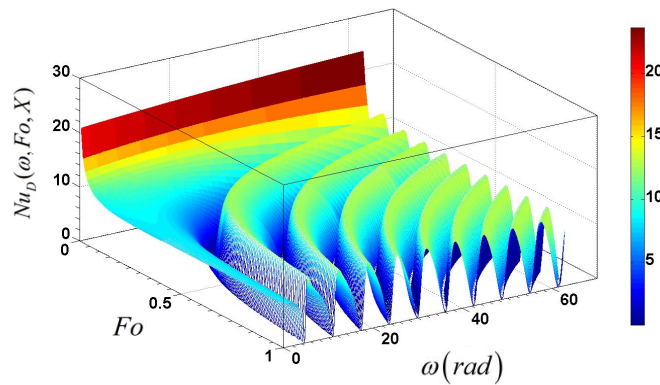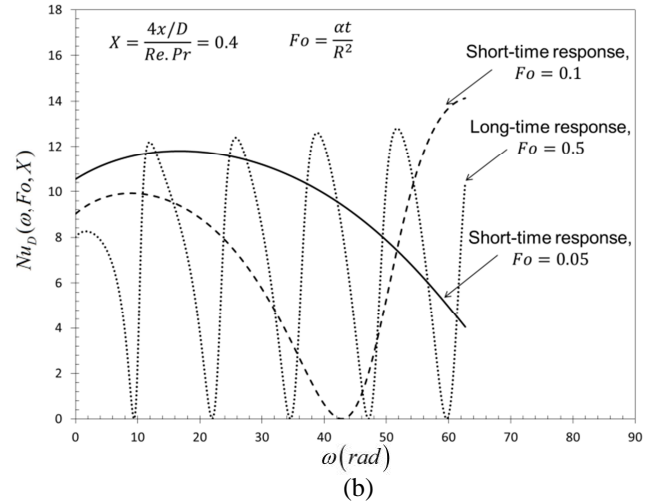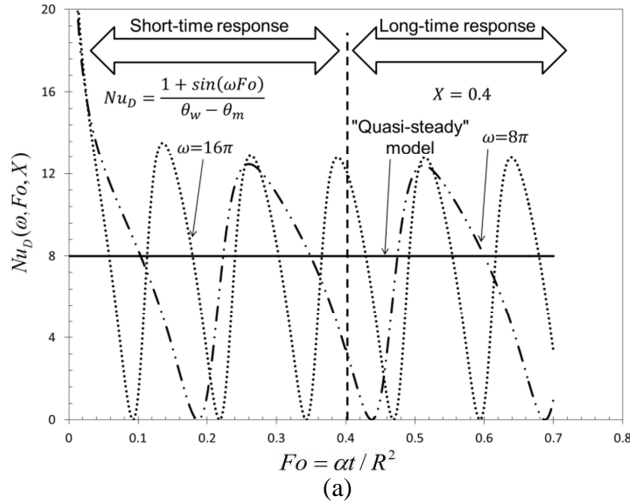
Figure 8 shows the variations of the local Nusselt number at a given axial position, $X = 0.4$, with the Fo number and the angular frequency, Eqs. (22) and (23). Regarding Fig. 8(a), the conventional "quasi-steady" model is a simplified model which assumes that the convective heat transfer coefficient is constant, equal to the fully developed condition in the channel [16].

The following can be concluded from Fig. 8:
- Changing the heat flux frequency alters the frequency of the Nusselt number. However, it does not change the amplitude of the Nusselt number considerably.
- The values of the transient Nusselt number deviate considerably from the ones predicted by the conventional quasi-steady model. The values of the Nusselt number predicted by Eqs. (22) and (23) can be 8 times lower than that of the quasi-steady model when the heat flux and hence the Nusselt number are zero. Therefore, the conventional models fail to predict the transient Nusselt number accurately.

- The Nusselt number oscillates slowly with the Fo number for small angular frequencies of the heat flux. Therefore, the values of the Nusselt number are higher than that of the cyclic heat flux with large angular frequencies over the entire range of the Fo number. Therefore, the optimum heat transfer occurs at very small values of the angular frequency. This will be discussed later in more details in this section.
- At initial times, the Nusselt number oscillates slowly with the angular frequency. This is corresponding to the slow fluctuations of the heat flux at initial times.
- As expected, increasing the angular frequency of the heat flux augments the frequency of the Nusselt number fluctuations. This happens due to the fact that the Nusselt number is zero at times in which the imposed cyclic heat flux is zero.

- Regardless of the angular frequency, at very initial transient period, the Nusselt number is much higher than that of the long-time response.
- At initial times, the values of the Nusselt number slightly increase with an increase in the angular frequency.

- The fluctuations of the transient Nusselt number occur around the fully-developed steady-state value. Considering the slug flow inside a circular tube, the value of the fully-developed Nusselt number for the steady-state condition is: $Nu_D = 8$ as predicted by the quasi-steady model [21].

(a)

(b)

(c)

Figure 8: Variations of the local Nusselt number at an arbitrarily-chosen axial position of $X = 0.4$ against (a): The Fourier number for different angular frequencies and comparison with the "Quasi-steady" model (b): the angular frequency for different Fourier numbers, and (c): the Fourier number and the angular frequency.

Depicted in Fig. 9 are the variations of a cyclic heat flux, $q'' = q_r''\left[1 + \sin\left(8\pi Fo\right)\right]$, and the corresponding Nusselt numbers of the fluid flow at a few axial positions along the tube.

The following highlights the trends in Fig. 9:
- At the inception of the transient period, the Nusselt number of all axial positions is only a function of time.

- The troughs of the Nusselt number at different axial positions are the same corresponding to the times at which the wall heat flux is zero.
- The values of the Nusselt number decrease at higher axial locations, i.e., further downstream. This is attributed to the boundary layer growth which insulates the tube wall, and reduces the rate of the heat transfer.
- For axial positions $X \geq 0.2$, the Nusselt number does not vary with an increase in axial position. This indicates that similar to the steady-state condition at $X = 0.2$, the boundary layers on the tube wall merge and the Nusselt number reaches its cyclic fully-developed value.

- As such, the thermally fully-developed region in transient internal forced convection, $X \geq 0.2$, can be defined as the region in which the Nusselt number does not vary with x any further, however; it can be an arbitrary function of time and the characteristics of the imposed heat flux.

Eq. (24) is developed in this study to predict the cyclic fully-developed Nusselt number with the Fourier number and the angular frequency. Regarding Eq. (24), the cyclic fully-developed Nusselt number is not a function of axial position. However, it fluctuates arbitrarily with time and the angular frequency.
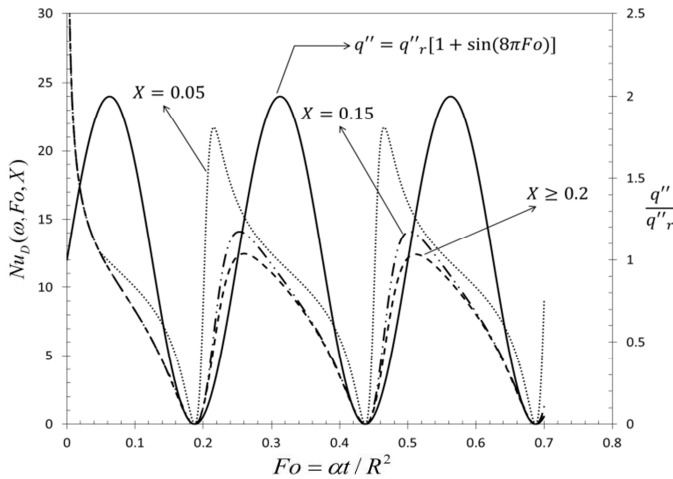

Figure 9. Variations of the applied heat flux,
$q'' = q''_r \left[1 + \sin\left(8\pi Fo\right)\right]$**, and the corresponding Nusselt number for a few axial positions along the tube.**
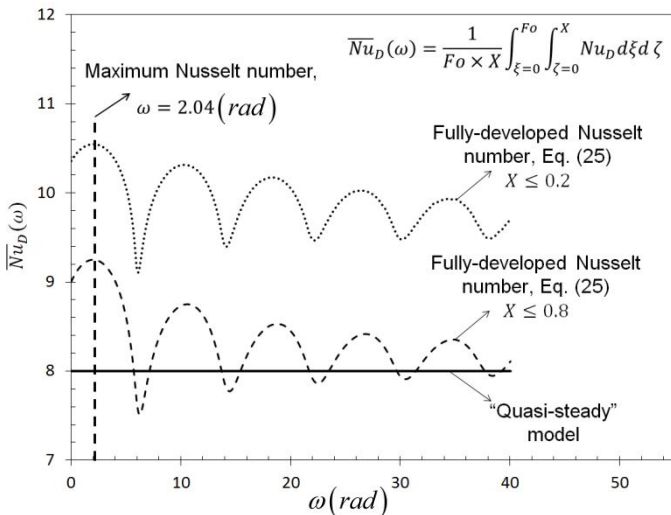

Figure 10: Variations of the average Nusselt number with the angular frequency and comparison with the quasi-steady model.

Variations of the average Nusselt number with the angular frequency are shown in Fig. 10, and compared with the quasi-steady model. Average entrance Nusselt number, $0 < X \leq 0.2$, and the average Nusselt number for an arbitrarily-chosen interval of $0 < X \leq 0.8$ are considered and the integral in Eq. (25) is carried out numerically for an arbitrary time interval of $0 < Fo \leq 0.8$.

One can conclude the following from Fig. 10,
- The average Nusselt number for a tube flow increases as the value of the axial position, $X = \dfrac{4x/D}{\text{Re.Pr}}$ decreases. This can be achieved by: i) decreasing the tube length; ii) increasing the tube diameter; iii) increasing the Reynolds number of the flow; and iv) using fluids with high Pr numbers such as oils.
- The maximum average Nu number occurs at the angular frequency of $\omega = 2.04\left(rad\right)$.
- The values of the averaged Nusselt number vary significantly with the angular frequency of the imposed heat flux, while the conventional models, e.g., quasi-steady model fail to predict such variations of the Nusselt number with time.
- The maximum average Nusselt number for the entrance region, $0 < X \leq 0.2$, evaluated by Eq. (25) is almost 21% higher than that of the quasi-steady model at the optimum value of the angular frequency i.e. $\omega = 2.04\left(rad\right)$.

7. CONCLUSION

A new full-time-range analytical model is developed to predict the transient thermal performance of forced-convective tube flow. Slug flow condition is considered for the velocity distribution inside a circular tube. To develop the model, the transient response for a step heat flux is considered, and generalized for an arbitrary time-dependent heat flux by a superposition technique i. e. Duhamel's integral. A prescribed cyclic time-dependent heat flux is considered and the thermal characteristics of the flow are obtained. As such, new all-time models are developed to evaluate: i) temperature distribution inside the fluid; ii) fluid bulk temperature; and iii) the Nusselt number. Furthermore, compact closed-form relationships are proposed to predict such thermal characteristics of the tube flow with the maximum relative difference of less than 10%. Optimum conditions are found to maximize the rate of the heat transfer in transient forced-convective tube flow.

The highlights of the present study can be listed as:
- For each axial position along the tube, there is an initial transient period of "pure-conduction-like" heat transfer in which the thermal characteristics of the tube flow is not a function of space and depends only on the time and the characteristics of the imposed heat flux, i.e. short-time response $X \geq Fo$.
- When $Fo = X$, the thermal response of the flow moves away from the pure-conduction response and adjusts towards a

steady oscillatory behavior at long-time response. This response remains the same all time thereafter, $X < Fo$; which depends on space, time, and the characteristics of the imposed heat flux.

- There is a thermal lag in the thermal response of the fluid temperature which increases towards the centerline of the tube due to the thermal inertia of the fluid.
- At the two limiting cases the thermal response of the fluid yields that of the step heat flux: i) $\omega \to 0$ and ii) $\omega \to \infty$.
- The short-time Nusselt number is much higher than that of the long-time response.
- The maximum average Nusselt number occurs at the angular frequency of $\omega = 2.04 (rad)$.
- For axial positions $X \geq 0.2$, the Nusselt number does not vary with an increase in axial position. At $X = 0.2$, the boundary layers on the tube wall merge and the Nusselt number reaches its cyclic fully-developed value.
- The thermally fully-developed region in transient internal forced convection, $X \geq 0.2$, is defined as the region in which the Nusselt number does not vary with x any further. However, it can be an arbitrary function of time and the characteristics of the imposed heat flux.
- Compact closed-form relationships are proposed to predict the i) tube-wall temperature; ii) fluid bulk temperature; and iii) the Nusselt number.

The obtained analytical results are verified successfully with the obtained numerical data. The maximum relative difference between the analytical results and the numerical data is less than 5.3%. It is also observed that the conventional quasi-steady model fail to predict the transient Nusselt number accurately.

NOMENCLATURE

ρ Density, (kg / m^3)

c_p heat capacity, $(J / kg.K)$

D Tube diameter, (m)

Fo Fourier number, $= \alpha t / R^2$

J Bessel function, Eq. (6)

k Thermal conductivity, $(W / m.K)$

$\dot{m}$ Mass flow rate, (kg / s)

Nu_D Nusselt number, $= hD / k$

Pr Prandtl number, (ν / α)

q'' Thermal load (Heat flux), (W / m^2)

$\dot{Q}$ Dimensionless heat flux, $= 1 / \theta_w$

u Velocity, (m / s)

x Axial distance from the entrance of the heated

r Radial coordinate measured from tube

R Tube radius, (m)

T Temperature, (K)

Re Reynolds number, $= UD / \nu$

t Time, (s)

X Dimensionless axial distance, $= 4x / Re.Pr.D$

Greek letters

α Thermal diffusivity, (m^2 / s)

ν Kinematic viscosity, (m^2 / s)

ρ Fluid density, (kg / m^3)

η Dimensionless coordinate, $= r / R$

θ Dimensionless temperature, $= \dfrac{T - T_0}{q_r'' D / k}$

φ Arbitrary function of X and Fo

β_n Positive roots of the Bessel function, Eq. (6)

ω Heat flux angular frequency, (rad / s)

ξ Dummy Fo variable

ζ Dummy X variable

Subscripts

0   Inlet

m Mean or bulk value

w wall

r Reference value

s Step heat flux

REFERENCES

[1] F. Agyenim, N. Hewitt, P. Eames, and M. Smyth, "A review of materials, heat transfer and phase change problem formulation for latent heat thermal energy storage systems (LHTESS)," *Renewable and Sustainable Energy Reviews*, vol. 14, no. 2, pp. 615–628, Feb. 2010.

[2] M. Hale, "Survey of thermal storage for parabolic trough power plants," *NREL report*, no. September, pp. 1–28, 2000.

[3] J. B. Garrison and M. E. Webber, "Optimization of an integrated energy storage for a dispatchable wind powered energy system," in *ASME 2012 6th International Conference on Energy Sustainability*, 2012, pp. 1–11.

[4] J. L. Sawin and E. Martinot, "Renewables Bounced Back in 2010, Finds REN21 Global Report," 2011.

[5]   T. I. TMC Press Release, "Cumulative Sales of TMC Hybrids Top 2 Million Units in Japan," 2012.

[6]   K. Bennion and M. Thornton, "Integrated vehicle thermal management for advanced vehicle propulsion technologies : Integrated Vehicle Thermal Management for Advanced Vehicle Propulsion Technologies," *NREL report*, pp. 1–15, 2010.

[7]   K. J. Kelly, T. Abraham, K. Bennion, D. Bharathan, S. Narumanchi, and M. O. Keefe, "Assessment of thermal control technologies for cooling electric vehicle power electronics," *NREL report*, no. January, 2008.

[8]   T. Kojima, Y. Yamada, and W. Fichtner, "A novel electro-thermal simulation approach of power IGBT modules for automotive traction applications," in *Proceedings of the 16th International Symposium on Power Semiconductor Devices & IC's*, 2004, no. v, pp. 289–292.

[9]   R. W. Johnson, J. L. Evans, P. Jacobsen, J. R. R. Thompson, and M. Christopher, "The changing automotive environment: high-temperature electronics," in *IEEE Transactions on Electronics Packaging Manufacturing*, 2004, vol. 27, no. 3, pp. 164–176.

[10]   M. Marz and A. Schletz, "Power electronics system integration for electric and hybrid vehicles," *Power Electronics*, pp. 16–18, 2010.

[11]   W.-R. Canders, G. Tareilus, I. Koch, and H. May, "New design and control aspects for electric vehicle drives," in *Proceedings of 14th International Power Electronics and Motion Control Conference EPE-PEMC 2010*, 2010.

[12]   E. M. Sparrow and R. Siegel, "Thermal entrance region of a circular tube under transient heating conditions," in *Third U. S. National Congress of Applied Mechanics*, 1958, pp. 817–826.

[13]   R. Siegel and E. M. Sparrow, "Transient heat transfer for laminar forced convection in the thermal entrance of flat ducts," *Heat Transfer*, vol. 81, pp. 29–36, 1959.

[14]   R. Siegel, "Transient heat transfer for laminar slug flow in ducts," *applied Mechanics*, vol. 81, no. 1, pp. 140–142, 1959.

[15]   R. Siegel, "Heat transfer for laminar flow in ducts with arbitrary time variations in wall temperature," *Applied Mec*, vol. 27, no. 2, pp. 241–249, 1960.

[16]   R. Siegel and M. Perlmutter, "Laminar heat transfer in a channel with unsteady flow and wall heating varying with position and time," *Trans. ASME*, vol. 85, pp. 358–365, 1963.

[17]   M. Perlmutter and R. Siegel, "Two-dimensional unsteady incompressible laminar duct flow with a step change in wall temperature," *Trans. ASME*, vol. 83, pp. 432–440, 1961.

[18]   R. Siegel, "Forced convection in a channel with wall heat capacity and with wall heating variable with axial position and time," *Int. J. Heat Mass Transfer*, vol. 6, pp. 607–620, 1963.

[19]   T. Von Karman and M. A. Biot, *Mathematical methods in engineering*. New York: McGraw-Hill, 1940, pp. 403–404.

[20]   "Fluent 6.3 User's Guide," Lebanon, 2007.

[21]   F. P. Incropera, D. P. Dewitt, T. L. Bergman, and A. S. Lavine, *Introduction to heat transfer*, Fifth. USA: John Wiley & Sons, 2007.